

DOI: 10.1002/cssc.201402397

Scalable Integration of Li_5FeO_4 towards Robust, High-Performance Lithium-Ion Hybrid Capacitors

Min-Sik Park,^[a] Young-Geun Lim,^[a, b] Soo Min Hwang,^[c] Jung Ho Kim,^{*[c]} Jeom-Soo Kim,^{*[a, d]} Shi Xue Dou,^[c] Jaephil Cho,^[e] and Young-Jun Kim^[a]

Lithium-ion hybrid capacitors have attracted great interest due to their high specific energy relative to conventional electrical double-layer capacitors. Nevertheless, the safety issue still remains a drawback for lithium-ion capacitors in practical operational environments because of the use of metallic lithium. Herein, single-phase Li_5FeO_4 with an antiferroite structure that acts as an alternative lithium source (instead of metallic lithium) is employed and its potential use for lithium-ion capacitors is verified. Abundant Li^+ amounts can be extracted from Li_5FeO_4 incorporated in the positive electrode and efficiently

doped into the negative electrode during the first electrochemical charging. After the first Li^+ extraction, Li^+ does not return to the Li_5FeO_4 host structure and is steadily involved in the electrochemical reactions of the negative electrode during subsequent cycling. Various electrochemical and structural analyses support its superior characteristics for use as a promising lithium source. This versatile approach can yield a sufficient Li^+ -doping efficiency of $> 90\%$ and improved safety as a result of the removal of metallic lithium from the cell.

Introduction

Lithium-ion hybrid capacitors (hereafter lithium-ion capacitors, LICs) have been considered as fascinating energy-storage systems in terms of specific energy density and power density because they exhibit higher power densities than rechargeable battery systems, such as lithium-ion batteries (LIBs), and higher energy densities than conventional electrical double-layer capacitors (EDLCs) through exploiting the advantages of both LIBs and EDLCs.^[1–3] Typically, LICs have an asymmetric configuration consisting of activated carbon as the positive electrode

(PE) and Li^+ -intercalated carbonaceous materials, such as graphite, as the negative electrode (NE). Such a hybrid cell configuration makes it possible to fully utilize its large capacity, and hence maximize the operational voltage up to ~ 4.2 V. This is much higher than that of conventional EDLCs (~ 3.0 V) due to the constant voltage behavior of close to 0 V during Li^+ insertion and extraction in the NE, consequently leading to the realization of electrochemical energy-storage systems with both high power and high energy densities.^[4–7] This advantage of LICs has shifted the focus of the research community on technical issues, such as further enhancement of performance, facile and cost-effective cell fabrication, and operational safety. Among the critical concerns, an efficient way to predope Li^+ ions into the NE is of great importance because Li^+ predoping is an essential process in the fabrication of commercial LICs.^[8–10] As a drawback, however, the hitherto inevitable use of metallic lithium needs to be handled with extra caution for safety in the fabrication and operation of the cells, owing to its high reactivity with moisture and poor tolerance of thermal shock, and thereby the possible occurrence of fire and explosions.

We have recently reported a new Li^+ -predoping approach using a stable lithium–transition metal oxide instead of metallic lithium for securing safety and controlling the extent of Li^+ doping in LICs.^[9,10] The integration of such an alternative lithium source into the PE has successfully allowed Li^+ ions to flow into the NE in a controllable manner by an electrochemical approach. These lithium–transition metal oxides must meet several electrochemical criteria to replace the use of metallic lithium and achieve advanced LICs. First, they should possess a large amount of available Li^+ ions in the unit structure, from which Li^+ is electrochemically extracted to act as the lithium

[a] Dr. M.-S. Park,⁺ Y.-G. Lim,⁺ Prof. J.-S. Kim, Dr. Y.-J. Kim
Advanced Batteries Research Center
Korea Electronics Technology Institute
68 Yatap-dong, Bundang-gu, Seongnam-si
Gyeonggi-do 463-816 (South Korea)
E-mail: js_energy@keti.re.kr


[b] Y.-G. Lim⁺
Department of Materials Science and Engineering
Korea University
5-1 Anam-dong, Seongbuk-gu, Seoul 136-713 (South Korea)

[c] Dr. S. M. Hwang, Prof. J. H. Kim, Prof. S. X. Dou
Institute for Superconducting and Electronic Materials
University of Wollongong
North Wollongong, NSW2500 (Australia)
E-mail: jhk@uow.edu.au

[d] Prof. J.-S. Kim
Department of Chemical Engineering, Dong-A University
840 Hadan2-dong, Saha-gu, Busan 604-714 (South Korea)
E-mail: jsenergy@dau.ac.kr

[e] Prof. J. Cho
School of Energy Engineering
Ulsan National Institute of Science and Technology
Ulsan 689-798 (South Korea)

[⁺] These authors contributed equally to this work.

 Supporting Information for this article is available on the WWW under <http://dx.doi.org/10.1002/cssc.201402397>.

source. Second, Li^+ extracted from the host material should not reversibly return to its former structure but be spontaneously involved in electrochemical reactions of the NE during cycling. In other words, the candidate materials must have a huge irreversibility in the first cycle to meet the requirements of the concept. Last, after Li^+ extraction, the delithiated phase of the host material in the PE should contribute in a limited way to the electrochemical reactions of LICs.

Taking those criteria into account, we propose herein Li_5FeO_4 (LFO) as a promising lithium source for robust, high-performance LICs for the first time. Antifluorite LFO that has been recently reported by Thackeray et al. as a possible cathode material in LIBs provides a large amount of Li^+ , with a capacity of $\sim 700 \text{ mAhg}^{-1}$ at the first cycle.^[11] Four Li^+ ions can be electrochemically extracted from a unit cell of LFO above 4 V versus Li/Li^+ by the partial oxidation of Fe^{3+} to Fe^{4+} , and extracted Li^+ does not reversibly return to its initial position during subsequent discharging, leading to poor initial coulombic efficiency at the first cycle.^[11] Even if such a characteristic of LFO would limit its practical use as a cathode material in LIBs, the irreversibility of Li^+ would raise another possibility for LICs. By capitalizing on the inherent characteristics of LFO, we theo-

retically designed an alternative to the otherwise inevitable use of metallic lithium for Li^+ predoping in LICs.

Results and Discussion

In contrast to the configuration of a pouch-type full cell of conventional LICs (Figure 1a, top right), which have an auxiliary metallic lithium electrode, a PE, and a NE, the LIC cell designed herein consists of a PE containing a small amount of single-phase LFO, together with activated carbon, and a NE without an auxiliary lithium electrode (Figure 1a, bottom right); Li^+ can be extracted from LFO in the PE and then incorporated into the NE, while forming the delithiated $\text{Li}_{5-x}\text{FeO}_4$ phase in the PE during the first electrochemical charging (Figure 1b, stage 1). Even after the first charge/discharge cycle (Figure 1b, stage 2), most of extracted Li^+ ions do not go back into $\text{Li}_{5-x}\text{FeO}_4$ in the PE, but still remains in the NE. During the following charge/discharge cycles (Figure 1b, stage 3), the remaining Li^+ ions do not participate in reversible reactions of LFO in the PE, but rather in anodic reactions in the NE.

To verify the utility of the proposed method to replace the use of metallic lithium for Li^+ predoping, we first synthesized

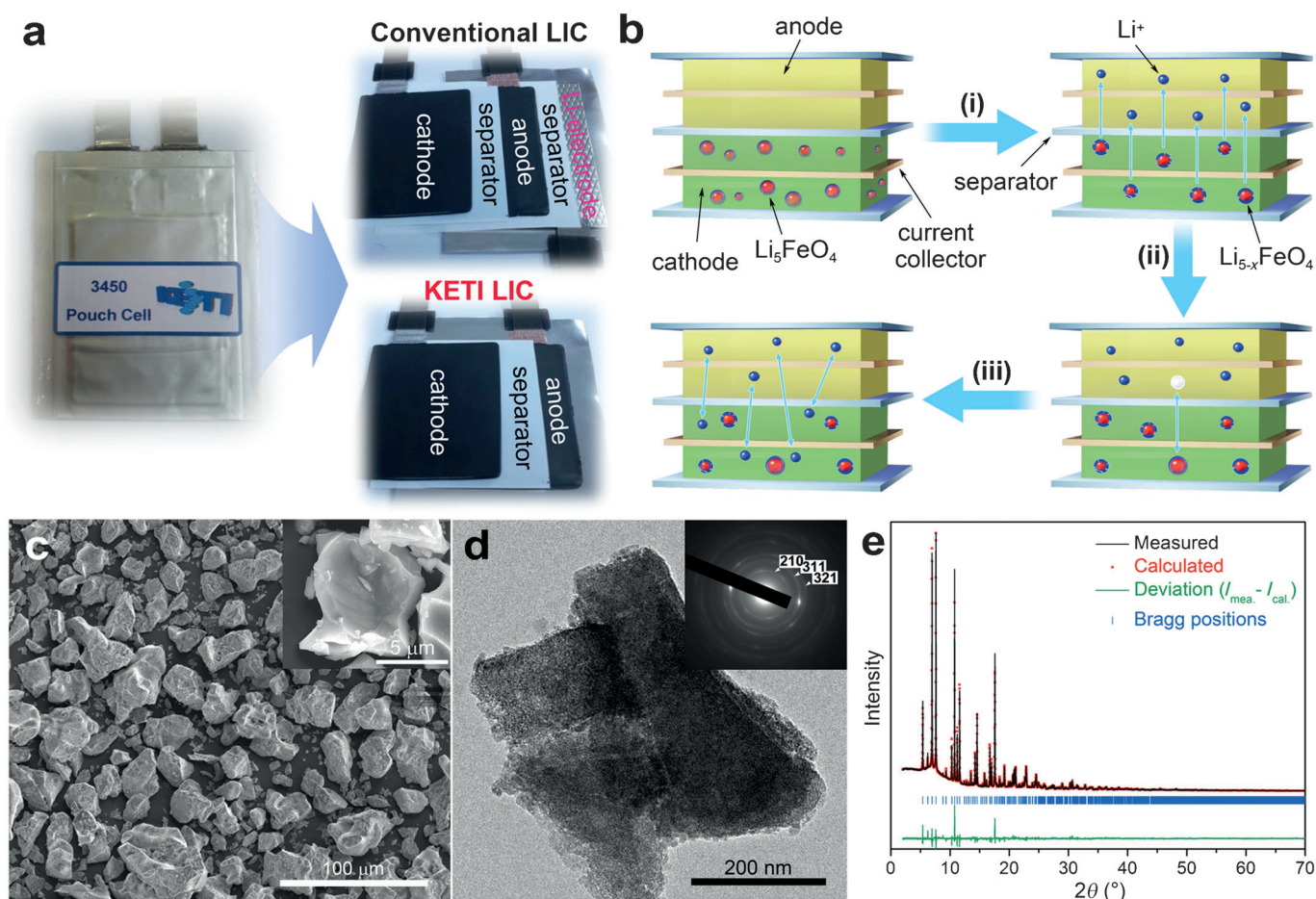


Figure 1. a) Comparison of full cell configurations: conventional LIC assembled with an auxiliary metallic Li electrode and LIC proposed by the Korea Electronics Technology Institute (KETI-LIC) containing Li_5FeO_4 as an alternative Li source in the positive electrode. b) Schematic diagram of the proposed Li^+ -predoping method using Li_5FeO_4 in the LIC. c) FESEM image of Li_5FeO_4 powder; inset: higher magnification image. d) TEM image of Li_5FeO_4 powder; inset: corresponding SAED pattern. e) Synchrotron X-ray diffraction pattern of Li_5FeO_4 powder with fine refinement results.

single-phase LFO powder by a solid-state reaction under optimized conditions. It has been reported that it is difficult to fabricate a pure LFO phase because it is vulnerable to moisture.^[12] In general, small amounts of impurity phases, such as α -LiFeO₂, are formed during synthesis. Through carefully controlling the synthetic conditions (e.g., temperature, heating rate, and atmosphere) during heat treatment, we obtained highly pure LFO particles. In field emission scanning electron microscope (FESEM) images (Figure 1b) LFO particles have sizes of a few tens of micrometers and an uneven particle shape. The surface of the sample is clean right after the synthesis (Figure 1c, inset). Through TEM analysis (Figure 1d), it is also found that the typical LFO single particle has an irregular shape and randomly oriented constituent nanocrystals with a size of 5–10 nm. The corresponding selected area electron-diffraction (SAED) pattern (Figure 1d, inset) shows a polycrystalline orthorhombic structure (see the Supporting Information, Figure S1a and b). Figure 1e presents the synchrotron X-ray diffraction (SXRD) pattern obtained from the LFO powder, together with the refinement results. All reflections are mainly indexed to the antiferroite structure, in which Fe³⁺ ions occupy tetrahedral sites and Li⁺ ions fill in the remaining tetrahedral sites. The structure has an orthorhombic symmetry,^[13,14] which belongs to space group *Pcab*, and the Li/Fe ratio of the sample is close to 5.04:1 as confirmed by inductively coupled plasma mass spectrometry (ICP-MS) measurements. The lattice parameters are calculated to be: $a=9.214$ Å, $b=9.206$ Å, and $c=9.169$ Å (see the Supporting Information, Table S1), which are close to the theoretical values ($a=9.218$ Å, $b=9.213$ Å, and $c=9.159$ Å).^[14] From refinement results, we confirmed that single-phase LFO powder was successfully synthesized without any secondary phase (e.g., α -LiFeO₂). This finding is also supported by an isothermal magnetization measurement (see the Supporting Information, Figure S1c): the *M*–*H* graph of the LFO sample shows typical paramagnetic behavior, indicating that

only Fe³⁺ occurs in the LFO lattice. As mentioned above, LFO powder easily tends to oxidize under ambient atmosphere, owing to its vulnerability to moisture, and thus much attention is required in handling; the white-colored LFO powder changed into a brown-colored powder after exposure to air for a day (see the Supporting Information, Figure S1d). The surface change is known to have resulted from the formation of LiOH·xH₂O.

From the viewpoint of safety, we further examined the thermal stability of the LFO powder at temperatures up to 1073 K (Figure 2a). According to high-temperature XRD patterns obtained up to 773 K, all reflections are well matched with that of single-phase LFO and there is no evidence for any impurity or secondary phase. Notably, LFO still maintains its own structure without any structural degradation up to 773 K. When the temperature exceeds 773 K, however, new additional peaks (Figure 2a, ▼) appear, which correspond to Fe₂O₃ (ICSD 10-8905).^[15] The results confirm that the LFO powder has excellent thermal stability up to 773 K. We further tested the thermal stability of LFO particles by using Mössbauer spectroscopy (Figure 2b). The Mössbauer spectra were collected from LFO powders at different temperatures, which indicate local environments of Fe atoms in a given structure. The spectrum acquired at 297 K consists of a doublet line, in which isomer shift (I.S.) and quadruple splitting (Q.S.) values were measured to be 0.13 and 0.95 mm s⁻¹, respectively, with a full width–half maximum (FWHM) value of 0.31 mm s⁻¹. Importantly, the obtained I.S. and Q.S. values are in agreement with typical Fe³⁺ ions in tetrahedra; other oxidation states of Fe were not detected in the spectra. Considering the fact that the I.S. and Q.S. values vary systematically as a function of oxidation, spin state, and coordination of Fe, it is found that the LFO sample does not contain any impurity.^[16] The spectra obtained from LFO at 323 and 373 K are almost the same as the room-temperature spectrum (297 K). There is no difference in the Q.S. value after stor-

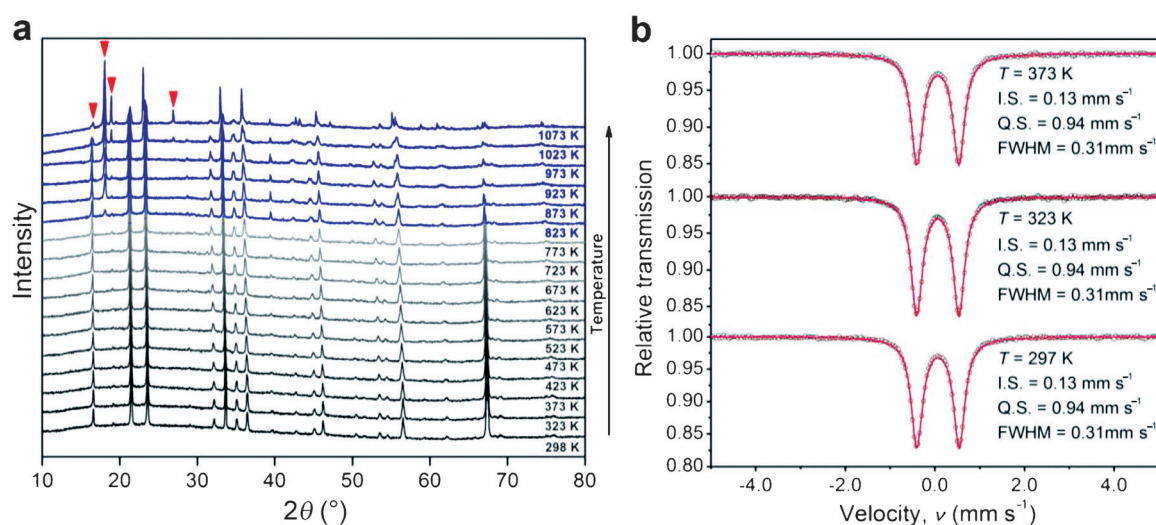


Figure 2. a) High-temperature powder X-ray diffraction patterns of Li₅FeO₄ powder at temperatures up to 1073 K; the temperature increases from the bottom to the top with a 50 K step. b) Mössbauer spectra collected from Li₅FeO₄ powders at 297, 323, and 373 K; calculated I.S. and Q.S. values are also provided.

age at high temperatures. This result reveals that the LFO powder is structurally stable even at the high temperature of 373 K.

Next, the irreversibility of Li intercalation from LFO during the first cycle (voltage range of 2.0 to 4.7 V vs. Li/Li⁺) was examined from the results of the corresponding galvanostatic voltage profile and in situ XRD patterns (Figure 3). With galvanostatic charging up to 4.7 V versus Li/Li⁺, two plateaus around 3.6 and 4.1 V versus Li/Li⁺ are observed (Fig-

worth emphasizing that around 84% of Li⁺ in LFO can be available for Li⁺ predoping of the NE without notable side reactions. One may argue that O₂ released from LFO during cycles is crucial for safety.^[11] In our proposed concept, it would not be serious because it is charged to high-voltage of 4.7 V versus Li/Li⁺ only once for the Li⁺ predoping process. After that, LIC is operated in a voltage window below 3.9 V and the delithiated LFO is not involved in electrochemical reactions anymore.

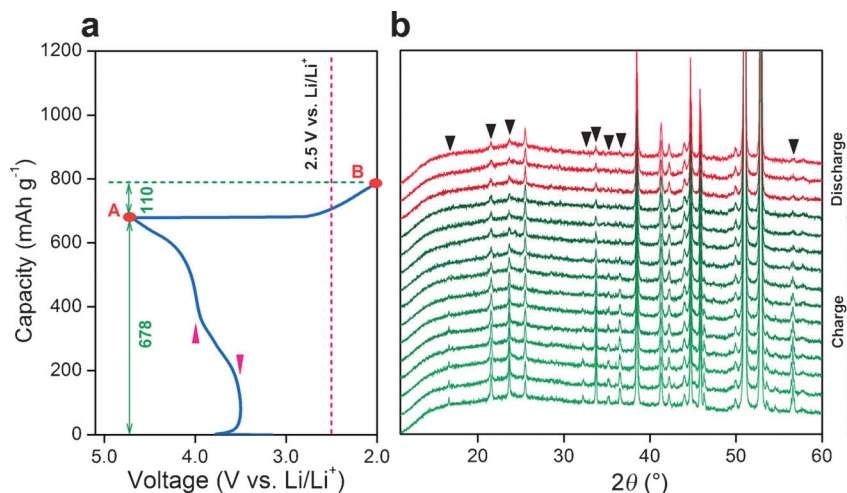


Figure 3. a) Galvanostatic voltage profile and b) corresponding in situ XRD patterns of optimized Li₅FeO₄ electrodes during the first cycle in the voltage range of 2.0 to 4.7 V versus Li/Li⁺; reflections are indexed to Li₅FeO₄ (▼), and other reflections originate from the Be window and the Al current collector. The first charge and discharge capacities are estimated to be ~678 mAh g⁻¹ (point A) and ~110 mAh g⁻¹ (difference between points B and A), respectively, as indicated by the triangles in Figure 3a.

ure 3a),^[11,17,18] which are in good accordance with the cyclic voltammogram, in which two distinctive peaks appear due to the oxidation of Fe³⁺ during the first cycle (see the Supporting Information, Figure S2). These results corroborate Li⁺ extraction from LFO through a two-step reaction at a given operating voltage window. The capacity delivered at the first charge is estimated to be ~678 mAh g⁻¹, which indicates that almost four Li⁺ ions are extracted from the host structure, with two Li⁺ ions extracted at each step, giving a capacity of ~339 mAh g⁻¹. Interestingly, the discharge capacity is ~110 mAh g⁻¹, revealing that only about 16% of extracted Li⁺ is recovered, that is, reversibly returns back to the LFO structure when the voltage is decreased to 2.0 V versus Li/Li⁺. This result suggests that about 84% of the Li⁺ ions extracted from LFO can be used for Li⁺ predoping. This large irreversibility of LFO mainly originates from the structural deformation caused by Li⁺ extraction from the host structure, as can be seen in in situ XRD patterns (Figure 3b). During the first charge, the intensities of the major reflections (Figure 3b, ▼) of LFO gradually decrease as Li⁺ extraction proceeds (charging).^[19] The LFO peaks do not recover, however, during the subsequent discharge to 2.0 V versus Li/Li⁺, indicating the huge irreversibility for Li⁺ insertion and extraction. Interestingly, secondary phases or impurities are not detected during the first cycle. It is also

For a rational cell design of an LIC employing the LFO, we investigated the fundamental properties of LFO as an alternative lithium source in LICs. First, the optimum cut-off voltage for the Li⁺-doping process was deduced to be 4.7 V versus Li/Li⁺ (see the Supporting Information, Figure S3). Second, to evaluate the controllable charging characteristics when LFO is incorporated into the PE, coin-type half cells containing PEs with different LFO contents were galvanostatically charged and discharged within a voltage range of 2.5 to 4.7 V versus Li/Li⁺. The applied charge current was fixed at 0.1 C (8.5 mA g⁻¹) for the first charge. The delivered charge capacity increases in proportion to LFO content, whereas the difference

negligible (see the Supporting Information, Figure S4). These results suggest that Li⁺ extraction can be controlled by adjusting the incorporated amount of LFO in the PE. In addition, it is speculated that the Li⁺ ions extracted from LFO is not involved in the reversible reaction of LFO but only in the anodic reaction of the NE after the first extraction from the host structure.

Based on the above electrochemical factors, the full LIC cell (Figure 1a) was carefully assembled through cell balancing of the PE and NE, and the electrochemical behavior of the LIC containing LFO (10.3 wt%) was compared to that of a conventional LIC. Figure 4a presents voltage profiles of the full cell (solid line) and the PE (dotted line) for the LIC containing LFO during the first charge to 4.7 V versus Li/Li⁺. Relative to the voltage profile of the LIC without LFO (dashed line), the LIC with LFO exhibits an additional charge capacity of ~0.40 mAh. The measured additional capacity is close to our design capacity (see the Supporting Information, Figure S5), and it appears to be a result of Li⁺ extraction from LFO incorporated in the PE. These findings confirm that Li⁺ ions can be extracted in a controlled manner for the Li⁺-doping process by the first electrochemical charging. The corresponding voltage profiles of the NE during the Li⁺-doping process are shown in Figure 4b, in which the voltage of the NE with LFO was recorded at 0.06 V versus Li/Li⁺ after the initial charge to 4.7 V versus Li/

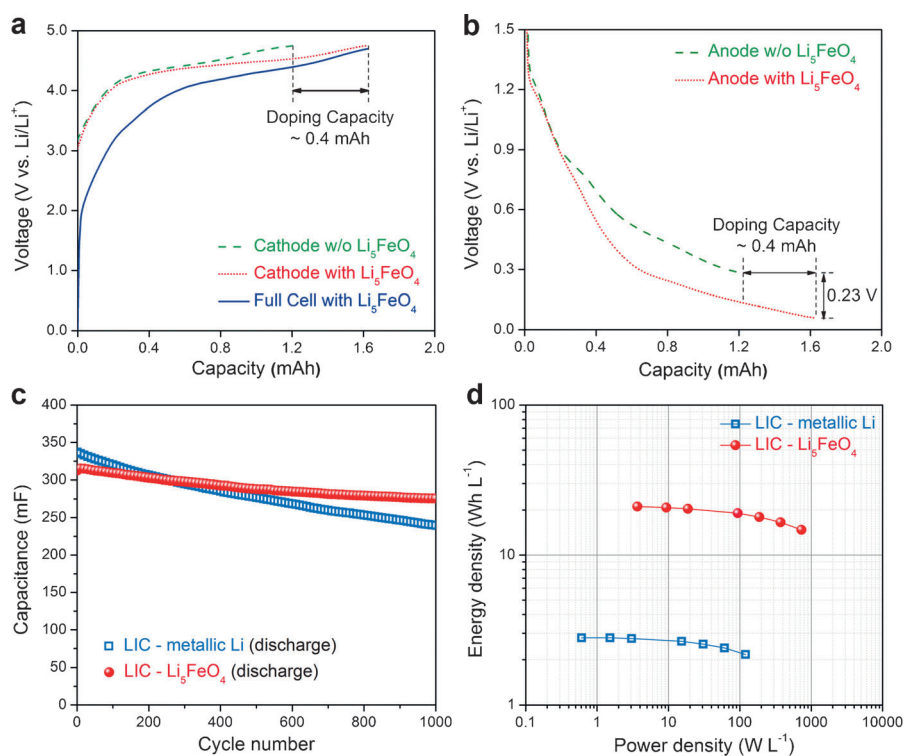


Figure 4. Galvanostatic voltage profiles of a LIC full cell assembled with a PE containing Li₃FeO₄ (10.3 wt %) a) in the positive electrode and b) in the negative electrode; c) cycling performance and d) Ragone plots of LIC full cells prepared by different Li⁺-predoping methods: the conventional method using metallic Li and the proposed method using Li₃FeO₄. LIC full cells were cycled in the voltage range of 1.5 to 3.9 V at a constant current of 10 C after Li⁺ predoping at a current density of 0.1 C. In the Ragone plots, data were plotted as a function of achieved capacitances at current densities of 0.2, 0.5, 1, 5, 10, 20, and 40 C.

Li⁺. The end-voltage of the LIC with LFO is 0.07 V, which is lower than that of the LIC without LFO. The voltage drop is responsible for the increase of 0.40 mAh in capacity in the case of Li⁺ insertion into the NE, which is well matched with the above voltage profile of the PE. Notably, Li⁺ ions extracted from LFO in the PE was incorporated into the NE without a significant loss. In addition, a much higher doping efficiency of 92.3% was attained by the proposed method using LFO. Generally, undesirable side effects in LICs result from side reactions with electrolytes or poor current uniformity due to metallic lithium that remains in the cell.^[20] In our approach, this issue could be considerably alleviated by employing LFO as an alternative lithium source. More importantly, the safety of LICs can be ensured and internal space in the cell is also saved, which enables a high volumetric energy density.

The rate capability of LICs containing LFO was compared with that of conventional LICs assembled with metallic lithium. Both LIC types show a similar discharging capacitance of ~380 mF at a low current density of 0.2 C (see the Supporting Information, Figure S6). When high currents are applied, LICs with LFO exhibit a slightly lower capacitance. At a current density of 40 C, the achieved capacitance of LICs containing LFO is estimated to be 268.3 mF, whereas it is 295.4 mF for LICs with metallic lithium. The difference in capacitance is reasonably explained by the addition of LFO into the PE, which increases the impedance of the electrode, and hence leads to a higher over-

potential of the PE in the LIC (see the Supporting Information, Figure S7). The slightly degraded capacity retention can be improved, however, by optimizing the particle size of LFO and by modifying electrode design (e.g., electrode composition and density).

The effect of LFO incorporation on cycling performance was also investigated in the voltage range of 2.5 to 3.9 V at a current density of 10 C after Li⁺ predoping (Figure 4c; see also the Supporting Information, Figure S8). LICs containing LFO have a slightly lower capacitance of ~315.2 mF at the initial cycle relative to LICs with metallic lithium due to the higher overpotential arising from the addition of LFO. The cyclic retention of LICs is notably improved, however, by the use of LFO. After 1000 cycles, LFO-containing LICs retain 87.4% (275.5 mF) of their initial capacity, whereas LICs with metallic lithium show a capacity retention of 71.1% (239.6 mF). To explore the origin

of the improvement of cyclic retention in LICs with LFO, we compared the voltage profiles of the PE and NE recorded from a four-electrode cell during cycling (see the Supporting Information, Figure S9). The voltages of the PE and NE in both LIC types gradually increase as cycling proceeds, which is possibly due to the depletion of Li⁺ involved in the anodic reaction during repeated cycles; Li⁺ depletion might have originated from degradation of the reversibility against Li⁺ insertion and extraction in the NE, as well as undesirable side reactions associated with the electrolyte during cycling. Relatively small increases in the voltage profiles of both PE and NE are observed for LICs containing LFO relative to LICs with metallic lithium. This improvement is attributed to a decrease in undesirable side reactions by employing LFO instead of metallic lithium, consequently leading to the more stable cycling performance of the LICs.

We constructed a Ragone plot based on measured capacitances at different current densities for the proposed LIC using LFO and the conventional LIC with metallic lithium (Figure 4d). In our suggested platform, eliminating metallic lithium for Li⁺ predoping allows for more internal space in the cell, which indicates that more electrochemical energy can be stored in the cells. It is highly advantageous from a technical viewpoint, therefore, to integrate LFO into the PE as an alternative lithium source instead of using metallic lithium. The proposed LIC shows a volumetric energy density (without power-density

fading) that is about four times higher relative to that of conventional LICs (see the Supporting Information, Figure S10). On the basis of the above electrochemical results, we emphasize that the proposed strategy of integrating LFO into the PE as a novel Li⁺ predoping method would be favorable not only for ensuring effective and controllable Li⁺ doping, good long-term cyclic performance, and enhanced volumetric energy density, but also for securing safety in fabrication and operation of LICs.

Conclusions

We rationally designed a lithium-ion hybrid capacitor (LIC) full cell by integrating single-phase Li₃FeO₄ (LFO) into the positive electrode (PE), without the use of metallic lithium for Li⁺ predoping, and thoroughly investigated its structural and electrochemical properties to explore the possibilities and limitations of LFO as an alternative lithium source for robust and high-performance LICs. The highly irreversibility extraction of Li⁺ from LFO, having a high capacity of ~700 mAh g⁻¹, is suitable for providing sufficient Li⁺ amounts for the NE prior to cell operation, and the doping level can be controlled in a scalable manner. By eliminating the auxiliary metallic lithium electrode and incorporating LFO into the PE in the cell, we achieved not only efficient Li⁺ predoping but also higher energy density and better safety of the LIC. Further optimizations, such as reducing the particle size of LFO and ensuring sufficient electrical conduction, would enhance the electrochemical performance of LICs and thereby assure the viability of the proposed facile but innovative approach.

Experimental Section

Sample preparation: Single-phase LFO was prepared by a solid-state reaction using lithium oxide (Li₂O, >97%, Aldrich) and iron (III) oxide (Fe₂O₃, >99%, Aldrich) as starting materials. Stoichiometric amounts of the starting materials were thoroughly mixed with a molar ratio of 5:1 and then physically ground. After grinding, the powder was pelletized and finally sintered at 900 °C under an Ar atmosphere for 48 h. The final product was a white-colored powder, which easily changed from white to orange when it was exposed to moisture. Therefore, the powder required careful handling in a dry room to prevent contact with moisture.

Structural characterizations: The structural analysis of LFO was directly confirmed by high-energy synchrotron radiation (SR) powder diffraction using a large Debye–Scherrer camera equipped with an imaging plate as a highly sensitive X-ray detector, at an experimental hutch of SPring-8, Japan. Magnetization (*M–H*) was estimated using a magnetic properties measurement system (MPMS). For this purpose, LFO powder (0.05431 g) was packed into a small capsule (0.13666 g) and was measured at 300 K. Isothermal magnetization was recorded by collecting a hysteresis loop between 50 and –50 kOe. Mössbauer measurements were performed up to 373 K. A γ -ray source of ⁵⁷Co in a Rh matrix of 925 MBq was used. The velocity scale of the spectra was relative to that of α -Fe at room temperature. The measurements of the source and the sample were conducted under the same temperature and pressure conditions ($P \approx 10^{-3}$ Pa). The structure of the final product was defined using an X-ray diffractometer (XRD, EMPYREAN, PAN analytical) equipped

with a 3D pixel semiconductor detector and CuK α radiation ($\lambda = 1.54056$ Å). In situ high-temperature XRD analyses were carried out with a scan step of 50 K under an air atmosphere. To collect in situ diffraction data, the cell was charged and discharged at a constant current density of 0.05 C in the voltage range of 2.5 to 4.7 V (vs. Li/Li⁺). Field emission scanning electron microscopy (FESEM, JEOL JSM-7000F) and high resolution transmission electron microscopy (HRTEM, JEOL JEM3010) were employed to examine the morphology and microstructure of the final product. In addition, the chemical state and composition of the final product were identified by X-ray photoelectron spectroscopy (XPS, Thermo Scientific Sigma probe) and inductively coupled plasma mass spectroscopy (ICP-MS, Bruker aurora M90), respectively.

Electrochemical measurements: The PE electrodes, composed of activated carbon and LFO, were prepared by coating a slurry containing the active materials (activated carbon+LFO, 92 wt%) and polyvinylidene difluoride (PVDF) as binder (8 wt%), dissolved in *N*-methyl-2-pyrrolidinone (NMP), on Al mesh. The NE was prepared by coating a slurry containing the active material (hard carbon, 80 wt%), conducting agent (super-P, 10 wt%), and binder (PVDF, 10 wt%) on Cu mesh. In the PE, the loading amount of LFO (10.3 wt%) was calculated based on the corresponding NE capacity (0.404 mAh; 60% doping level) and the specific capacity of LFO (673 mAh g⁻¹) when it is charged up to 4.7 V (vs. Li/Li⁺). The fractions of active (activated carbon) and additive (LFO) mass were designed to amount to 81.7 and 10.3 wt%, respectively. The loading level and density of the PE were fixed at 6.1 mg cm⁻¹ and 0.5 g cm⁻³. To evaluate electrochemical properties, beaker-type half cells and full cells were carefully assembled in a dry room. The PE and NE were punched into disks $\varnothing 12$ and $\varnothing 14$ mm in size, respectively, and electrolyte (8 mL) was added into each cell. A porous polyethylene membrane was used as the separator, and LiPF₆ (1.3 M) dissolved in ethylene carbonate/dimethyl carbonate (3:7 v/v, PANAX ETEC Co. Ltd) was used as the electrolyte. For Li⁺ predoping, the cells were charged to 4.7 V (vs. Li/Li⁺) and discharged to 2.5 V (vs. Li/Li⁺) with a constant current rate of 0.1 C. After that, the cells were further cycled in a voltage range of 1.5 to 3.9 V at different current densities.

Acknowledgements

This research was supported by the Converging Research Center Program through the Ministry of Science, ICT and Future Planning, Korea (2013K000290). This work was also partially supported by the IT R&D program of MOTIE/KEIT [10046306, Development of Li-rich Cathode (≥ 240 mAh g⁻¹) and Carbon-free Anode Materials (≥ 1000 mAh g⁻¹) for High Capacity/High Rate Lithium Secondary Batteries].

Keywords: capacitors · doping · electrochemistry · electrodes · lithium

- [1] G. G. Amatucci, F. Badway, A. D. Pasquier, T. Zheng, *J. Electrochem. Soc.* **2001**, *148*, A930.
- [2] A. Yoshino, T. Tsubata, M. Shimoyamada, H. Satake, Y. Okano, S. Mori, S. Yata, *J. Electrochem. Soc.* **2004**, *151*, A2180.
- [3] H. Wang, M. Yoshio, A. K. Thapa, H. Nakamura, *J. Power Sources* **2007**, *169*, 375.
- [4] Y. Zhang, H. Feng, X. Wu, L. Wang, A. Zhang, T. Xia, H. Dong, X. Li, L. Zhang, *Int. J. Hydrogen Energy* **2009**, *34*, 4889.

- [5] T. Aida, I. Murayama, K. Yamada, M. Morita, *J. Electrochem. Soc.* **2007**, *154*, A798.
- [6] A. Burke, *Electrochim. Acta* **2007**, *53*, 1083.
- [7] K. Naoi, S. Ishimoto, J. Miyamoto, W. Naoi, *Energy Environ. Sci.* **2012**, *5*, 9363.
- [8] S. R. Sivakkumar, A. G. Pandolfo, *Electrochim. Acta* **2012**, *65*, 280.
- [9] M. S. Park, Y. G. Lim, J. H. Kim, Y. J. Kim, J. Cho, J. S. Kim, *Adv. Energy Mater.* **2011**, *1*, 1002.
- [10] M. S. Park, Y. G. Lim, J. W. Park, J. S. Kim, J. W. Lee, J. H. Kim, S. X. Dou, Y. J. Kim, *J. Phys. Chem. C* **2013**, *117*, 11471.
- [11] C. S. Johnson, S. H. Kang, J. T. Vaughey, S. V. Pol, M. Balasubramanian, M. M. Thackeray, *Chem. Mater.* **2010**, *22*, 1263.
- [12] L. Liang, J. Luo, M. Chen, L. Wang, J. Li, X. He, *Int. J. Electrochem. Sci.* **2013**, *8*, 6393.
- [13] S. P. Ong, L. Wang, B. Kang, G. Ceder, *Chem. Mater.* **2008**, *20*, 1798.
- [14] R. Luge, R. Hoppe, *Z. Anorg. Allg. Chem.* **1984**, *513*, 141.
- [15] L. Ben-Dor, E. Fischbein, Z. H. Kalman, *Acta Crystallogr. Sect. B* **1976**, *32*, 667.
- [16] A. Hirano, T. Matsumura, M. Ueda, N. Imanishi, Y. Takeda, M. Tabuchi, *Solid State Ionics* **2005**, *176*, 2777.
- [17] N. Imanishi, Y. Inoue, A. Hirano, M. Ueda, Y. Takeda, H. Sakaebe, M. Tabuchi, *J. Power Sources* **2005**, *146*, 21.
- [18] M. N. Obrovac, R. A. Dunlap, R. J. Sanderson, J. R. Dahn, *J. Electrochem. Soc.* **2001**, *148*, A576.
- [19] N. Imanishi, A. Hirano, M. Ishihara, M. Ueda, Y. Takeda, M. Tabuchi, presented at *Proc. the 204th Meeting of the Electrochemical Society (ECS)*, Orlando, Florida, October **2003**, 379.
- [20] D. Aurbach, E. Zinigrad, Y. Cohen, H. Teller, *Solid State Ionics* **2002**, *148*, 405.

Received: May 9, 2014

Published online on September 10, 2014